RSC Advances

ROYAL SOCIETY OF CHEMISTRY

www.rsc.org/advances

Synthesis of a functionalized fibrous adsorbent of high uptake capacity: A study on Pb(II) uptake and simple acidic site model development

Vihangraj V. Kulkarni[1], Animes Kumar Golder[*2] and Pranab Kumar Ghosh[1]

[1]Department of Civil Engineering, Indian Institute of Technology Guwahati

[2]Department of Chemical Engineering, Indian Institute of Technology Guwahati

[*]Corresponding author

Phone: +91-3612582269

Fax: +91-3612582291

Email: animes@iitg.ernet.in

Abstract

The breakdown of lignin barrier by acid treatment could expose cellulosic functional groups on the surface of biomaterials. In this study, a new functionalized fibrous adsorbent (FFA) was prepared using arecanut (*Areca catechu*) husk in sulfuric acid media. The synthesized FFA was characterized using proximate & ultimate analyses, thermogravimetric analysis (TGA), Brunauer-Emmett-Teller (BET) surface area, scanning electron microscopy (SEM), energy dispersive X-ray (EDX) and Fourier transform infrared (FTIR) spectroscopy. A simple dual-site proton adsorption (DSPA) model was developed and applied for equilibrium Pb(II) uptake on the basis of mass balance. The quantity of proton absorbed onto FFA, obtained from potentiometric titrations, was used to determine the acid dissociation constants (pK_a) and the concentration of functional groups. The model fitted parameters showed a great agreement to the experimental results. The FTIR spectra and also the pK_a values of 3.21 and 1.62, respectively, confirmed the presence of surface carboxylic and sulfonic groups. FFA exhibited significant Pb(II) uptake and the Pb(II) ions predominantly attached to the carboxylic group even though the concentration was about 25% lower than the sulfonic group. FFA with a dose of 1 g L^{-1} showed around 98.3% Pb(II) removal at pH 5 from an initial concentration of 32 mg L^{-1} (0.157 mM). It could be used for 12 cycles with the exhaustion capacity of 194.94 mg g^{-1} of FFA which was about 3.4 times higher than the commercial activated carbon.

Keywords: Lignocellulose material; Functionalized adsorbent; Potentiometric titration; Lead removal

1 Introduction

The presence of heavy metals in the environment are a major concern due to its persistent and non-biodegradable nature.[1] In general, toxic metals attack the active sites of the enzymes and inhibit the essential enzymatic activity. They are also dangerous because they tend to bio-accumulate.[2, 3] Adsorption techniques for heavy metals removal possess many advantages such as simplicity in design & operation and reuse of spent adsorbent. Activated carbon (AC) is one of the most common adsorbents used for heavy metal uptake.[4, 5] Although various low-cost adsorbents, namely, chitosan,[6] zeolites,[7] mineral clays,[8] coir pith,[9] peanut husk,[10] jute fibres, sawdust,[11] sludge solids[12] and rice husk[13] were also used for metal removal after surface modification by various chemical and/or thermal processes. However, the reports on the use of arecanut husk and its surface modification for heavy metal removal from contaminated water is scanty.

India is the largest consumer and producer of arecanut (betel nut), responsible for 52.8% of global production. In India, Karnataka, Kerala and Assam holds about 83% in terms of cultivation area and production of arecanut. Assam is the 3rd highest producer among them.[14] The endosperm of arecanut is a principal chewing material in eastern countries like India, Bangladesh, Malaya, Ceylon and Japan. [15, 16] The lignocellulosic husk covering the chewing material (endosperm), is thrown away in environment which constitutes about 60 to 80% of the total weight of arecanut. [17] However, there are limited studies on the utilization of arecanut husk for the preparation of hick board, plastics and wrapping paper etc. [14, 18] Acid treatment of such lignocellulose is an established procedure in the field of biofuel production and various other uses.[19, 20] Acid breaks the lignin seal and disrupts the hydrogen bonding between cellulose making it more accessible.[19] High temperature (160-220 °C) during acid treatment hydrolyses hemicellulose increasing the porosity of biomaterial.[21] Although arecanut husk contain about 44% cellulose, 28% hemicellulose and 11% lignin,[22] its use as a

feedstock for biofuel production is limited due to its high ash content and lower susceptibility to enzymatic digestion.[22] Arecanut husk is found to be an efficient adsorbent for Pb(II) removal after its functionalization using Fenton reagent with a Fe^{2+}/H_2O_2 ratio of 0.01.[23]

Adsorption mostly takes place in the pores of an adsorbent or on the surface functional groups. Natural materials carry various surface functional groups such as carboxylic, sulfonic, phosphatic and phenolic groups.[24] Functionalization and surface modification of an adsorbent improve the capacity and/or desired properties for a specific application. Therefore, modification of different low-cost materials such as biomass, agricultural materials as well as solid wastes is carried out using mineral and organic acids.[25] An improved Pb(II) uptake capacity of peanut husk is reported by HCl mediated modification.[10] Treatment of sawdust with sulphuric acid followed by soaking in sodium bicarbonate resulted in the formation of carboxylic groups on its surface. It showed an increase in maximum Cu(II) adsorption capacity of 13.49 mg g^{-1} against 5.43 mg g^{-1} by untreated sawdust.[26]

In this study, a new functionalized fibrous adsorbent (FFA) was synthesized using arecanut husk by sulphuric acid treatment. It was characterized in terms of proximate & ultimate analyses, TGA, BET surface area, SEM, FTIR and EDX spectroscopies. A simple equilibrium dual-site proton adsorption (DSPA) model was developed, and dissociation constants of acidic sites present onto FFA were determined using potentiometric titration. FFA was used for Pb(II) removal from aqueous solution and DSPA model was applied to uncover Pb(II) binding to the active acidic sites. Furthermore, the performance of FFA was compared with a commercial activated carbon (CAC) as a reference adsorbent, for Pb(II) uptake.

2 Materials and Methods

2.1 Reagents

Milli-Q water (resistivity less than 15 MΩ cm) was used to prepare all standard and stock solutions (Millipore S.A.S., Molsheim, France). Chemicals used in this study were either of analytical reagent (AR) or laboratory reagent (LR) grades. Lead nitrate (minimum assay 99%) was procured from S.D. Fine Chemicals, Mumbai. Sodium nitrate (99% purity), potassium bromide (purity 99%), sulphuric acid (minimum assay 98%) and sodium hydroxide (minimum assay 98%) were procured from Loba Chemie, India.

2.2 Preparation of FFA

The precursor, arecanut husk, was collected from local trading shops at nearby IIT Guwahati campus, Assam, India. It was washed with tap water to remove adhered particles, dirt and dried for 24 h at 70 °C in a hot air oven (International Commercial Traders, Kolkata, India). The husk was manually cut into small pieces (length of 0.3-0.5 cm), for faster functionalization. The dried husk pieces are termed as the raw fibrous adsorbent (RFA). 150 g of RFA was taken in a 2 L borosilicate glass container and required amount of concentrated H_2SO_4 (98%) was added to make mass to volume ratio (RFA: H_2SO_4 acid) of 1:2 (w/v).[1, 27, 28] It was swirled with the help of a glass rod. The content of beaker reached to around 120 °C due to exothermic reaction between the acid and RFA. The temperature gradually dropped to 105 °C in 20 min, and the beaker was then kept in a hot air oven at the same temperature for 2 h.[29, 30] Acid treated husk thus prepared was washed with distilled water for several times until the pH of wash water became 5.00±0.10. It was then dried at 105 °C to get functionalized fibrous adsorbent (FFA). FFA particles were screened using Indian Standard sieves. Particles passed through 1000 µm sieve and retained on 300 µm sieve were collected and, stored in a desiccator for further experimentation.

2.3 Batch adsorption experiment

All the batch adsorption studies were performed in 250 ml borosilicate conical containers with Pb(II) spiked 100 ml Milli-Q water and agitated at 180 rpm in an incubator shaker (LSI-1005R, Lab Tech, India) with a fixed FFA dosage of 1 g L^{-1} unless and otherwise specified. The experiments were conducted at varying initial pH between 1 and 5 at 30 °C. Initial pH of the solution was not raised beyond 5 to avoid Pb(II) precipitation at higher pH [31] as well as reduction of active sites of FFA. Sulfuric acid and sodium hydroxide solution of suitable strengths were used to adjust solution pH (μpH System-361, Systonic, India). The samples were withdrawn at regular intervals of time, filtered through Whatman filter paper (# 41) and analyzed for residual Pb(II) concentration in an Atomic Absorption Spectrometer (AAS) (55 B, Spectra AA Varian, Australia).

In this study, the uptake capacity of the adsorbent refers to the maximum amount of metal uptake in one cycle at a fixed initial metal concentration. The metal uptake capacity, was determined by varying the initial Pb(II) concentration from 25 to 200 mg L^{-1} with 1 g L^{-1} FFA at an initial pH 5. The exhaustion capacity was calculated from cumulative uptake capacities from all cycles till the exhaustion. In order to determine the exhaustion uptake capacity using Eq. 1, the spent FFA was reused for multiple cycles. After each cycle, FFA was filtered out through Whatman filter paper (# 41), washed with distilled water and oven-dried at 105 °C for 2 h. The recovered FFA was then used in the next adsorption cycle with the fresh Pb(II) solution.

$$\text{Metal uptake capacity of FFA, } \text{mg g}^{-1} = \frac{\sum_{i=1}^{12}[C_o - C_e]_i \times V}{m} \qquad (1)$$

Where, i = number of cycles, C_o = initial Pb(II) concentration (mg L^{-1}) is same for all the cycles, C_e = final Pb(II) concentration (mg L^{-1}) from individual cycle, V = volume of Pb(II) solution treated (L), and m = mass of FFA (g).

The performance of FFA for Pb(II) removal was compared with the commercial activated carbon (CAC), as a reference adsorbent. The BET surface area of CAC was determined using N_2 adsorption−desorption isotherm at -196 °C (ASIQM0000-4, Autosorb IQ, Quantachrome Instruments, USA). The identical experimental condition with the various initial Pb(II) concentration as that of FFA for Pb(II) removal was also used in the case of CAC.

2.4 Potentiometric titration

The nature of the functional groups and its concentration was determined by the potentiometric titration.[32-34] It is based on the hypothesis that each site is occupied by the titratable protons. In this study, the potentiometric titration was carried out by suspending 0.05 g of FFA in 50 mL 0.1 N sodium nitrate solution.[32] pH was first adjusted to 2, and FFA was added. It was then agitated overnight at 180 rpm and 30 °C in an incubator shaker to reach the equilibrium. The titration was performed with 0.5 N NaOH using a precision automated titrator (DL60, Mettler Toledo, Switzerland). The number of titratable surface protonated acidic groups was determined from the difference between the bulk proton concentration in the presence and in the absence of FFA.[32]

2.5 Characterization of FFA and RFA

The ultimate analysis of FFA and RFA was done using CHNS Elemental Analyzer (EA3000, Eurovector, Italy) by taking 1 mg of sample in a tin boat assortment for determination of percentage composition of carbon, hydrogen, sulfur and nitrogen. The percentage oxygen was determined by means of difference.[22] Thermogravimetric analysis (TGA 209F1D-0179-L, Netzsch, Germany) was performed by heating the sample under nitrogen atmosphere between 30 and 700 °C with a ramping rate of 10 °C min^{-1}. For

proximate analysis, 25 g sample (as received) was put into an oven-dried moisture free crucible equipped with a lid, and heated up to 575 °C in a muffle furnace (RMF 46/14, Reico Equipments and Instruments, Kolkata, India) for 3 h. The volatile solids (Eq. 2) and moisture content (Eq. 3) on wet basis were estimated as described in USEPA method 1684.

$$\text{Volatile solids, } \% = \frac{(m_2 - m_3)}{(m_1 - m_0)} \times 100 \quad (2)$$

$$\text{Moisture content, } \% = 100 - \frac{m_1 - m_2}{m_1 - m_0} \times 100 \quad (3)$$

Where, m_0= empty weight of crucible, m_1= m_0+ sample weight as received, m_2= m_0+ sample weight after drying at 105 °C, m_3= m_0+ sample weight after drying at 575 °C. The ash content (%) on wet basis was expressed as = 100 - volatile solids - moisture content.

FTIR spectra (PE-RXI, Perkin-Elmer, USA) were recorded to identify the functional groups on the surface of both RFA and FFA. Scanning electron microscope (SEM) (Leo, 1430 vp, Carl Zeiss, Germany) images were acquired to observe the surface texture of adsorbents. Energy dispersive X-ray spectroscopy (EDX) analysis (Leo, 1430 vp, Carl Zeiss, Germany) was employed for further confirmation of Pb(II) uptake by FFA.

3 Development of DSPA model

FFA predominantly contains two acidic sites i.e. carboxylic and sulfonic groups (as outlined in sections 4.1.3 & 4.3). The dissociation reaction of carboxylic acid can be written as in Eq. 4.[32]

$$\equiv COOH \leftrightarrow \equiv COO^- + H^+ \quad (4)$$

Where, the symbol "≡" indicates the surface of the adsorbent to which the functional groups are attached, $\equiv COOH$ and $\equiv COO^-$ are protonated and dissociated carboxylic acid at equilibrium.

The acid dissociation constant K_1 (M) can be expressed as in Eq. 5.

$$K_1 = \frac{[\equiv COO^-][H^+]}{[\equiv COOH]} \quad (5)$$

The total concentration of carboxylic sites (N_1, M) at any point of time can be given as (Eq. 6):

$$N_1 = [\equiv COOH] + [\equiv COO^-] \quad (6)$$

The equilibrium protonated carboxylic site concentration can be expressed as in Eq. 7 by rearranging Eqs. 5 and 6.

$$[\equiv COOH] = N_1 \left[\frac{[H^+]}{[H^+]+K_1}\right] \quad (7)$$

Similarly for protonated sulfonic site as is in Eq. 8.

$$[\equiv SO_3H] = N_2 \left[\frac{[H^+]}{[H^+]+K_2}\right] \quad (8)$$

Therefore, the total pronated acidic site concentration ($N_{P,total}$, mol g^{-1}) is given by Eq. 9.

$$N_{P,total} = N_1 \left[\frac{[H^+]}{[H^+]+K_1}\right] + N_2 \left[\frac{[H^+]}{[H^+]+K_2}\right] \quad (9)$$

The equilibrium metal (M^{2+}) adsorption in solution can be described as

$$\equiv COO^- + M^{2+} \leftrightarrow \equiv COOM^+ \quad (10)$$

The metal binding constant, K_{M1} can be written as (Eq.11):

$$K_{M1} = \frac{[\equiv COOM^+]}{[\equiv COO^-][M^{2+}]} \quad (11)$$

Further the concentration carboxylic group in presence of M^{2+} (with M^{2+} binding) can be expressed as in Eq. 12

$$N_1 = [\equiv COOH] + [\equiv COO^-] + [COOM^+] \quad (12)$$

The Eq. 13 can be obtained by substituting $[\equiv COOH]$ and $[\equiv COO^-]$ from Eqs. 7 and 11

$$N_1 = [COOM^+]\left[\frac{K_1K_{M1}[M^{2+}]+[H^+]+K_1}{K_1K_{M1}[M^{2+}]}\right] \quad (13)$$

Similarly for sulfonic site and total metal attached to both the sites q_e, (mol g^{-1}) can be expressed as Eq. 14

$$q_e = \left[\frac{N_1 K_1 K_{M1}[M^{2+}]}{K_1 K_{M1}[M^{2+}]+[H^+]+K_1}\right] + \left[\frac{N_2 K_2 K_{M2}[M^{2+}]}{K_2 K_{M2}[M^{2+}]+[H^+]+K_2}\right] \quad (14)$$

4 Results and Discussion

4.1 Physicochemical properties of adsorbents

4.1.1 Proximate & ultimate analyses, TGA and BET surface area

The results of proximate and ultimate analyses of RFA and FFA are shown in Table S1 of the Supplementary Material. RFA contained about 2.93% ash, 6.4% moisture and high amount of volatile matter. After acid treatment, ash and volatile matter increased and moisture content decreased. C and S content in FFA increased slightly compared to RFA. The increase in S content was attributed to toting of sulfonic functional groups, later confirmed by FTIR and potentiometric titration. The similar trend of ash content for both RFA and FFA also can be seen from the TGA at 700 °C (Fig. S1 of the Supplementary Material). The greater weight loss for FFA than RFA up to 280 °C was noticed, and it was higher after that for RFA. The results of differential thermogravimetric analysis for RFA (Fig. S2 of the Supplementary Material) showed three major grooves at 280, 325 and 500 °C, referring to decomposition of hemicellulose, cellulose and lignin, respectively. Hemicellulose and cellulose degradation usually start at around 206 and 315 °C, respectively, while lignin decomposition begins above 330 °C.[22] The results obtained in the present study well match with the degradation pattern of lignocellulosic materials such as bonbogori, moz, bagasse and cashew shell.[22, 35]

For FFA, there was only a little increase in BET surface area with acid treatment (Table S1). However, both RFA and FFA gave notably lower surface area compared to activated carbon and activated alumina.[5] The BET surface area, pore volume and average pore size of CAC were found as 646.7 m^2 g^{-1}, 0.442 cm^3 g^{-1} and 2.158 nm, respectively. The lower temperature attained (max 120 °C) while FFA synthesis melted the crystalline part of

hemicellulose and removed it partially. Hence, surface area did not increase much. Higher synthesis temperature was avoided as it could hydrolyze hemicellulose completely but may cause loss of lignin and cellulose content[21, 36] which may in turn reduce a total number of acidic site present.

4.1.2 SEM images and EDX spectra

The surface of RFA appeared to be very smooth having no cracks. The small ridges of lignocellulosic materials on the surface of RFA were arranged in a regular fashion (Fig. S3 of the Supplementary Material). Whereas, the surface of fresh FFA is highly uneven with a few irregular pores and cracks on its surface owing to acid treatment (Figs. 1a and 1b). Acid treatment of RFA caused swelling of husk resulting in the formation of pores and cracks due to a destruction of lignocellulosic structure and partial hydrolysis of hemicellulose.[19, 21] Similar results are reported for nitric acid treated bael fruit shell.[37] The surface appeared to be sticky after Pb(II) adsorption, and no pore was visible (Figs. 1c and 1d) indicating that all the pores were occupied by Pb(II). Pb(II) loading onto FFA estimated by EDX analysis (Fig. S4 of the Supplementary Material) and experimentally were within ±5%.

4.1.3 FTIR spectra

FTIR spectra of FFA before Pb(II) adsorption shows higher transmittance in the range of 3500 to 3700 cm^{-1} (Fig. 2). The peak appearing at 3606 cm^{-1} is likely to be attributed to hydrogen bonded alcohol group over a broader stretch and higher intensity. These groups is supposed to yield from glucoside linkage of cellulose or hydroxyphenyl and syringyl groups of lignin. The similar results for arecanut husk are also reported.[22] The peak near 1700 cm^{-1} for most of the carbonaceous biomass materials possesses C=C stretching absorption frequency.[24, 38] FTIR spectra confirmed the presence of C=O stretch of α, β unsaturated -

COOH group originating from deeper oxidation of part of alcoholic hydroxyl groups of lignin present on RFA identified from the peak at 1705 cm^{-1} (Fig. S5 of the Supplementary Material).[39] The peak at 1400 cm^{-1} can be recognized as C-O stretch of -COOH group. The band due to O-H stretching vibration of hydrated sulfonic acid is very broad having several maxima in the regions between 1650 and 2800 cm^{-1}. The peak at 1168 cm^{-1} can be attributed to SO_3 asymmetric stretching vibrations. The shift of peaks from 3606 to 3620, 2350 to 2357, 1705 to 1731 and 1168 to 1198 cm^{-1} were noticed after Pb(II) adsorption (Fig. 2). It clearly demonstrates significant affinity of Pb(II) towards sulfonic and carboxylic groups. However, protonation and deprotonation plays a major role in the affinity behavior of Pb(II) to different acidic groups.

4.1.4 Potentiometric titration and buffering capacity of FFA

Fig. 3a shows the titration curve for FFA against the cumulative volume of 0.5 N NaOH added. The shift of the titration curve towards right-side with FFA can be seen. It is evident that the solution with FFA showed buffering capacity confirming the release of protons into bulk solution (Fig. 3b). The progressive dissociation of protonated sites was observed as titration continued. The titration curve of FFA was not so distinguishable to locate the equivalence points referring to neutralization of each acidic groups.[40] It signifies that FFA is composed of many titratable functional groups dissociated with pH elevation. The change in solution pH was referred solely to the exchange of protons between FFA and the bulk solution. Similar results for the characterization of oxidized AC are also reported.[41] However, almost no deflection in the titration curve was observed in the case of RFA. Likewise, it overlapped with the titration curve with no adsorbent (Fig. 3a).

The buffering capacity of the FFA was calculated by the difference in volume of NaOH need to be added to reach pH 12, with and without FFA. The buffering capacity of

FFA with 1 g L^{-1} dosage was found to be 1.88×10^{-2} mol g^{-1}. The functionalized adsorbents prepared using the dead biomass of *B. subtillis* and *S. oneidensis* showed the buffering capacities of 2.8×10^{-4} and 3.1×10^{-4} mol g^{-1} with the dosage of 75-150 and 50 g L^{-1}, respectively.[42] A higher buffering capacity of FFA in comparison with the dead microorganisms refers to the presence of strongly accessible acidic sites on the surface of FFA, releasing protons. Fig. 3b shows the variation of equilibrium pH with respect to initial pH in the absence of Pb(II). FFA displayed an unusual buffering capacity in the pH range of 2.8 to 3.1 for initial pH from 3 to 10. On the other hand, RFA didn't show the buffering capacity as in accordance with the titration curve (Fig. 3a).

4.2 Application of FFA for Pb(II) uptake

In this study, a range of FFA was synthesized by varying the concentration of H_2SO_4. The assortment of adsorbents was based on the performance in Pb(II) removal. FFA prepared with 24, 48, 72 and 98% H_2SO_4 showed Pb(II) removal efficiencies of 28, 36, 42 and 98.3%, respectively, from an initial Pb(II) concentration and pH of 32 mg L^{-1} and 5. The diluted H_2SO_4 could only breach the lignin walls partially and, so the lower Pb(II) uptake was noted.[24] Hence, the subsequent studies were carried out with the FFA prepared using the highest strength of acid.

In a detailed study, the initial pH of the solution was varied from 1 to 5 to study its effects on the kinetics of Pb(II) uptake. The concentration of H^+ ion is a crucial factor for Pb(II) uptake as the dissociation of acidic sites as well as the metal chemistry strongly depends on it.[43, 44] The studies targeting effect of pH on Pb(II) speciation reported that at pH< 6, Pb^{2+} is the predominant species. Above pH 6 lead exists as $Pb(OH)^+$ and $Pb(OH)^0_2$ hence, removal could also be by precipitation of $Pb(OH)^0_2$ and sorption of $Pb(OH)^+$.[31] The effect of contact time on Pb(II) uptake is shown in Fig. 4. Negligible Pb(II) uptake capacity of 1.39 mg

g^{-1} was observed for RFA; whereas it was 31.47 mg g^{-1} for FFA both at pH 4 and 5 (Fig. 4a). The rate of Pb(II) binding was faster during first 30 min, reduced afterward and the uptake began to plateau after 5 h. The fall in uptake rates can be explained on the basis of concentration gradient and availability of active acidic sites.

The decrease in Pb(II) removal (Fig. 4b) at lower pH can be explained with possible two reasons. Firstly, in acidic range there is a competition between Pb(II) and H^+ ions for the same binding sites which inhibits Pb(II) removal. Similar results in the removal of heavy metals have been reported by various researchers.[9, 11, 44] The second reason is on the basis of surface complexation at lower pH. Protonation of chelating groups reduces complexation with available ligands and hence the percentage uptake decreases.[45] The optimum pH was taken as 5 based on experimental results of Pb(II) uptake and literature reported on speciation of Pb(II). Hence, all further experiments were carried out at pH 5 to avoid possible precipitation of Pb(II).[31] It is also necessary to mention that the final pH of the solution was about 3.1 (Fig. 4b) for all the experiments irrespective to the initial pH using FFA. The reduction in solution pH indicates that removal of Pb(II) ions was facilitated by ion exchange i.e. H^+ ion was released from functional groups present on FFA. A similar phenomenon in the removal of Cr(III) using cation exchanger is reported.[46] Removal of Cd(II) by nitric acid modified corncob also confirmed ion exchange as removal mechanism.[47]

The results of FFA exhaustion study are shown in Fig. 5. It can be seen that in first adsorption cycle almost 100% Pb(II) was removed from an initial concentration of 32 mg L^{-1} (0.157 mM). The high Pb(II) removal continued in the second cycle also, with little decrease wherein removal of 97% was achieved. Second cycle onwards, after every cycle, gradual decrease in Pb(II) removal was observed. Removal of Pb(II) became insignificant after 12 cycles. The FFA gave a very high exhaustion capacity of 194.94 mg g^{-1} in 12 cycles (calculated using Eq. 1) as compared to adsorbents prepared by acid treatment using

biomaterial (Table S2 of the Supplementary Material). It renders the use of FFA especially in a continuous mode of operation for practical applications.[48] Almost the whole amount of FFA used in the adsorption study was recoverable. So the mass loss due to repeated washing and drying was found to be insignificant (< 1 % in 12 cycles).

In order to compare the performance of FFA and CAC, the uptake capacities were determined, and the results are shown in Fig. S6 of the Supplementary Material. The higher uptake capacity at the elevated initial concentration was due to the stronger driving force between the bulk solution and active sites of the FFA. In case of CAC, the uptake capacity was improved when the initial concentration of Pb(II) was increased. But beyond 125 mg L^{-1}, the increment was insignificant, indicating the exhaustion of CAC. Whereas, the uptake capacity of FFA was increased almost linearly till the highest initial concentration of 200 mg L^{-1} used in this study. Pb(II) uptake of 92 mg g^{-1} FFA was increased by 31% by increasing the initial concentration from 125 to 200 mg L^{-1}. The uptake capacities of FFA and CAC with 200 mg L^{-1} initial concentration of Pb(II) were 118.66 and 56.79 mg g^{-1}, respectively. The results of this study imply fairly high capacity and significant superiority of FFA over CAC in Pb(II) removal.

4.3 DSPA model and its evaluation for Pb(II) binding

Protonation characteristics of FFA were obtained from the difference between the bulk proton concentration with and without FFA. FFA usually stabilizes the solution pH around 3.2. The different equilibrium pH (Figs. 6 and 7) was adjusted through repeated addition of either 6 N H_2SO_4 or NaOH. The acidic sites concentration was determined using DSPA model given by Eq. 9. K_1, K_2 and N_1, N_2 refer to dissociation constants and total number (mol g^{-1}) of each functional group. The model constants were estimated by fitting the results obtained in potentiometric titration using GRG nonlinear regression analysis (solver

tool of Microsoft Office Excel 2013). The experimental and model fitted (R-squired value of 0.98) values of N_p (mol g^{-1}) are presented in Fig. 6a. The model showed an excellent agreement with the experimental data. The FFA was containing two major functional groups with pK_{a1} and pK_{a2} values of 3.21 and 1.62, respectively, corresponding to strongly acidic groups.[41] The surface functional groups possess the same pK_a values as of their organic acids and; pK_{a1} and pK_{a2} could be assigned to carboxylic and sulfonic groups, respectively.[41, 49] The total concentration of carboxylic groups was 25% lesser than that of sulfonic groups and it was calculated to be 1.53×10^{-3} and 2×10^{-3} mol g^{-1}. Availability of a particular acidic site for metal adsorption is dependent upon protonation and deprotonation which in turn is a function of pH. Percentage distribution of protonated sites at various solution pH is shown in Fig. 6b. With rise in pH, protonation of sulfonic sites decreased and that of carboxyl sites increased. Weakly acidic carboxylic group (pK_{a1} 3.21) were available partially (protonated 40-50%) for Pb(II) binding below pH 3.2. Whereas rise in pH above 3.21 enriched protonated site concentration and thereby increasing available Pb(II) sorptive sites. Availability of carboxylic sites for Pb(II) binding was higher than sulfonic sites at pH > 1.2. Sulfonic sites were available partially for Pb(II) removal, particularly at higher proton concentration (Fig. 6b). Similar results for contribution of sulfonate groups to heavy metal biosorption are reported.[50] They found that the contribution of sulfonate groups in heavy metal removal was little but could be significant at higher proton concentration.

Equilibrium binding model (Eq. 14) was employed to reveal the binding nature of Pb(II) with functional sites. Pb(II) removal data at different equilibrium pH was fitted to find out Pb(II) binding constants of K_{M1} and K_{M2} for carboxylic and sulfonic sites, respectively. The model exhibited great agreement with the experimental results (Fig. 7a). K_{M1} and K_{M2} were found to be 5.20×10^{6} and 28.11 L mol^{-1}, respectively. Fig. 7b shows contribution of carboxylic and sulfonic group for Pb(II) binding. It can be observed that at all pH values

carboxylic group was mostly involved in Pb(II) binding and sulfonate group exhibited negligible Pb(II) uptake. Removal of Pb(II) was because of its strong affinity towards carboxylic group. Sulfonic groups gave only an uptake of 6.4 mg g^{-1} (0.031 mM g^{-1}) of FFA at pH 2 indicating that little Pb(II) removal could be possible at lower pH. The similar results for sulfonate groups of raw and modified biomass of *Sargassum fluitansare* are reported in literature.[50] They investigated both qualitative and quantitative contribution of carboxylic and sulfonic functional groups for uptake of Cd(II) and Pb(II) by selective esterification method. Plette and coworkers also showed predominant Cd(II) bounding to carboxylic sites than phosphatic of a gram-positive soil bacterium.[51]

5 Conclusions

The study draws an important conclusion on induction of functional groups using sulphuric acid treatment onto lignocellulosic biomaterial i.e. arecanut husk and its behaviour for Pb(II) uptake. The presence of carboxylic and sulfonic groups was identified by FTIR spectra and confirmed by DSPA model derived parameters using potentiometric titration. Acid functionalized husk exhibited a bit higher sulphur content which was consistent with EDX spectra and higher asymmetric stretching vibrations of SO_3. The uneven and porous texture developed became sticky and barely porous after Pb(II) adsorption. Highly acidic pH found to be indigent for Pb(II) removal, however, almost 100 % removal was achieved at pH 5. The adsorbent could be used, as many as 12 times, and the exhaustion capacity found to be 194.94 mg g^{-1} at pH 5, for which the contribution of carboxylic groups was much higher. Pb(II) uptake using FFA was around twice than a commercial activated carbon. The possible mechanism of Pb(II) removal was supposed to be ion exchange which was confirmed by lower pH of the solution after adsorption. pK_a values and concentration of carboxylic and sulfonic groups were of 3.21, 1.62 and 1.53×10^{-3}, 2×10^{-3} mol g^{-1}, respectively. Synthesised

FFA showed a buffering capacity of 1.88×10^{-2} mol g^{-1} at a dosage of 1 g L^{-1}. Pb(II) binding constants (K_M) were found to be 5.2×10^{6} and 28.11 L mol^{-1} for carboxylic and sulfonic sites, respectively with overall binding constant of 1.46×10^{8} L mol^{-1}.

References

1. M. Kobya, E. Demirbas, E. Senturk and M. Ince, *Bioresour. Technol.*, 2005, **96**, 1518-1521.
2. E. B. Hart, H. Steenbock, J. Waddell and C. A. Elvehjem, *Nutr. Res.*, 1987, **45**, 181-183.
3. A. Srivastava, S. S. Peshin, T. Kaleekal and S. K. Gupta, *Hum. Exp. Toxicol.*, 2005, **24**, 279-285.
4. A. Jusoh, L. Su Shiung, N. a. Ali and M. J. M. M. Noor, *Desalination*, 2007, **206**, 9-16.
5. K. C. Kang, S. S. Kim, J. W. Choi and S. H. Kwon, *J Ind Eng Chem*, 2008, **14**, 131-135.
6. A. T. Paulino, L. B. Santos and J. Nozaki, *React. Funct. Polym.*, 2008, **68**, 634-642.
7. S. R. Taffarel and J. Rubio, *Miner. Eng.*, 2010, **23**, 1131-1138.
8. G. Y. Hsu, R. M. Wu, D. J. Lee and J. C. Liu, *Water Res.*, 1999, **33**, 248-256.
9. K. Kadirvelu, K. Thamaraiselvi and C. Namasivayam, *Bioresour. Technol.*, 2001, **76**, 63-65.
10. S. Ricordel, S. Taha, I. Cisse and G. Dorange, *Sep. Purif. Technol.*, 2001, **24**, 389-401.
11. B. Yu, Y. Zhang, A. Shukla, S. S. Shukla and K. L. Dorris, *J. Hazard. Mater.*, 2001, **84**, 83-94.
12. K. M. Smith, G. D. Fowler, S. Pullket and N. J. D. Graham, *Sep. Purif. Technol.*, 2012, **98**, 240-248.
13. S. Babel and T. A. Kurniawan, *J. Hazard. Mater.*, 2003, **97**, 219-243.
14. B. T. Ramappa, *IOSR-JAVS*, 2013, **3**, 50-59.
15. K. N. Arjungi, *Arzneimittelforschung*, 1976, **26**, 951-956.
16. P. C. Gupta and S. Warnakulasuriya, *Addiction Biology*, 2002, **7**, 77-83.
17. A. Rajan, J. G. Kurup and T. E. Abraham, *Biochem. Eng. J.*, 2005, **25**, 237-242.
18. R. Raghupathy, R. Viswanathan and C. T. Devadas, *Bioresour. Technol.*, 2002, **82**, 99-100.
19. N. Mosier, C. Wyman, B. Dale, R. Elander, Y. Y. Lee, M. Holtzapple and M. Ladisch, *Bioresour. Technol.*, 2005, **96**, 673-686.
20. H.-J. Huang, S. Ramaswamy, W. W. Al-Dajani and U. Tschirner, *Bioresour. Technol.*, 2010, **101**, 624-631.
21. V. Chaturvedi and P. Verma, *3 Biotech*, 2013, **3**, 415-431.
22. S. Sasmal, V. V. Goud and K. Mohanty, *Biomass Bioenergy*, 2012, **45**, 212-220.
23. X.-m. Li, W. Zheng, D.-b. Wang, Q. Yang, J.-b. Cao, X. Yue, T.-t. Shen and G.-m. Zeng, *Desalination*, 2010, **258**, 148-153.
24. R. S. Bai and T. E. Abraham, *Water Res.*, 2002, **36**, 1224-1236.
25. W. S. Wan Ngah and M. A. K. M. Hanafiah, *Bioresour. Technol.*, 2008, **99**, 3935-3948.
26. F. N. Acar and Z. Eren, *J. Hazard. Mater.*, 2006, **137**, 909-914.
27. H. S. Altundogan, N. Bahar, B. Mujde and F. Tumen, *J. Hazard. Mater.*, 2007, **144**, 255-264.
28. E. Demirbas, M. Kobya, S. Öncel and S. Şencan, *Bioresour. Technol.*, 2002, **84**, 291-293.
29. P. Alvarez, C. Blanco and M. Granda, *J. Hazard. Mater.*, 2007, **144**, 400-405.
30. D. Sivakumar, *Global Journal of Environmental Science and Management*, 2015, **1**, 27-40.
31. D. Xu, X. Tan, C. Chen and X. Wang, *J. Hazard. Mater.*, 2008, **154**, 407-416.

32. M. K. Gagrai, C. Das and A. K. Golder, *Can. J. Chem. Eng.*, 2013, **91**, 1904-1912.
33. H. Seki and A. Suzuki, *J. Colloid Interface Sci.*, 1998, **206**, 297-301.
34. M. Villen-Guzman, A. Garcia-Rubio, J. M. Paz-Garcia, J. M. Rodriguez-Maroto, F. Garcia-Herruzo, C. Vereda-Alonso and C. Gomez-Lahoz, *Electrochimica Acta*, DOI: http://dx.doi.org/10.1016/j.electacta.2015.03.061.
35. K. Umamaheswaran and V. S. Batra, *Fuel*, 2008, **87**, 628-638.
36. F. Xu, Y.-C. Shi and D. Wang, *Bioresour. Technol.*, 2013, **135**, 704-709.
37. J. Anandkumar and B. Mandal, *J. Hazard. Mater.*, 2009, **168**, 633-640.
38. I. A. W. Tan, A. L. Ahmad and B. H. Hameed, *J. Hazard. Mater.*, 2008, **154**, 337-346.
39. Suhas, P. J. M. Carrott and M. M. L. Ribeiro Carrott, *Bioresour. Technol.*, 2007, **98**, 2301-2312.
40. G. Sanna, G. Alberti, P. Castaldi and P. Melis, *Fresenius Environ. Bull.*, 2002, **1**, 636-641.
41. M. Joao Paulo de, B. M. Patricia and G. Honoria de Fatima, *J. Braz. Chem. Soc*, 2006, **17**.
42. L. A. Seders and J. B. Fein, *Chem. Geol.*, 2011, **285**, 115-123.
43. D. Chauhan and N. Sankararamakrishnan, *Bioresour. Technol.*, 2008, **99**, 9021-9024.
44. J. T. Nwabanne and P. K. Igbokwe, *Int. J. Eng. Res. Appl.*, 2012, **2**, 1830-1838.
45. D. Fanou, B. Yao, S. Siaka and G. Ado, *J. App.l Sci.*, 2007, **7**, 310-313.
46. T. S. Anirudhan and P. G. Radhakrishnan, *J. Colloid Interface Sci.*, 2007, **316**, 268-276.
47. R. Leyva-Ramos, L. A. Bernal-Jacome and I. Acosta-Rodriguez, *Sep. Purif. Technol.*, 2005, **45**, 41-49.
48. L. D. Benefield, J. F. Judkins and B. L. Weand, *Process chemistry for water and wastewater treatment*, Prentice-Hall, 1982.
49. R. E. Martinez, D. S. Smith, E. Kulczycki and F. G. Ferris, *J. Colloid Interface Sci.*, 2002, **253**, 130-139.
50. E. Fourest and B. Volesky, *Environ. Sci. Technol.*, 1995, **30**, 277-282.
51. A. C. C. Plette, M. F. Benedetti and W. H. van Riemsdijk, *Environ. Sci. Technol.*, 1996, **30**, 1902-1910.

List of Figure Captions

Fig. 1 SEM images of FFA before Pb(II) adsorption: 164X (a) and 410X (b). SEM images of FFA after Pb(II) adsorption (Pb(II) loading 75 mg g^{-1} FFA, temperature 30 °C, agitation speed 180 rpm and contact time 5 h): 1000X (c) and 2000X (d) magnifications.

Fig. 2 FTIR spectra of virgin and Pb(II) loaded FFA (initial Pb(II) concentration 100 mg L^{-1}, adsorbent dosage 1 g L^{-1}, agitation speed 180 rpm, temperature 30 °C, contact/ equilibrium time 5 h).

Fig. 3 (a) Titration curves with and without adsorbent. **(b)** Variation of equilibrium pH without Pb(II) (FFA and RFA dosage 1 g L^{-1}, temperature 30 °C and agitation speed 180 rpm).

Fig. 4 (a) Kinetics of Pb(II) using RFA and FFA as a function of contact time at different initial pH, and **(b)** Percentage removal of Pb(II) at equilibrium (contact time 5 h, initial Pb(II) 32 mg L^{-1} (0.157 mM), FFA dose 1 g L^{-1}, temperature 30 °C and agitation speed 180 rpm).

Fig. 5 Removal of Pb(II) in cyclic batch adsorption study by FFA (Pb(II) 32 mg L^{-1} (0.157 mM), FFA dose 1 g L^{-1}, temperature 30 °C and agitation speed 180 rpm).

Fig. 6 Determination of acid dissociation constants using DSPA model (Eq. 9) (FFA dosage 1 g L^{-1}, agitation speed 180 rpm, temperature 30 °C). **(a)** Number of protonated sites (in absence of Pb(II)) determined from potentiometric titration and model fitting (RMSE 6.01×10^{-5}, SD 3.61×10^{-9}, SSE 2.56×10^{-7}). **(b)** Percentage distribution of protonated carboxylic and sulfonic sites in titrated pH range.

Fig. 7 (a) Equilibrium Pb(II) removal at different pH: Experimental vs. model fitted (Eq. 14). **(b)** Contribution of each functional group in Pb(II) binding (FFA dosage 1 g L^{-1}, agitation speed 180 rpm, temperature 30 °C).

List of Figures

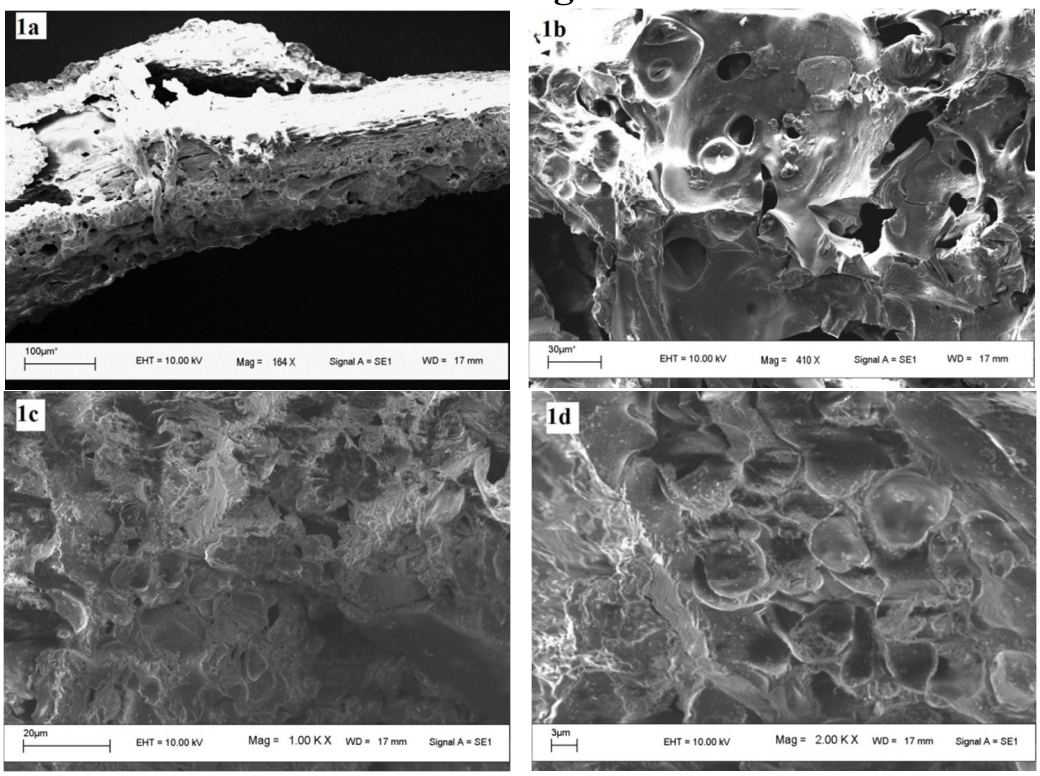

Fig. 1

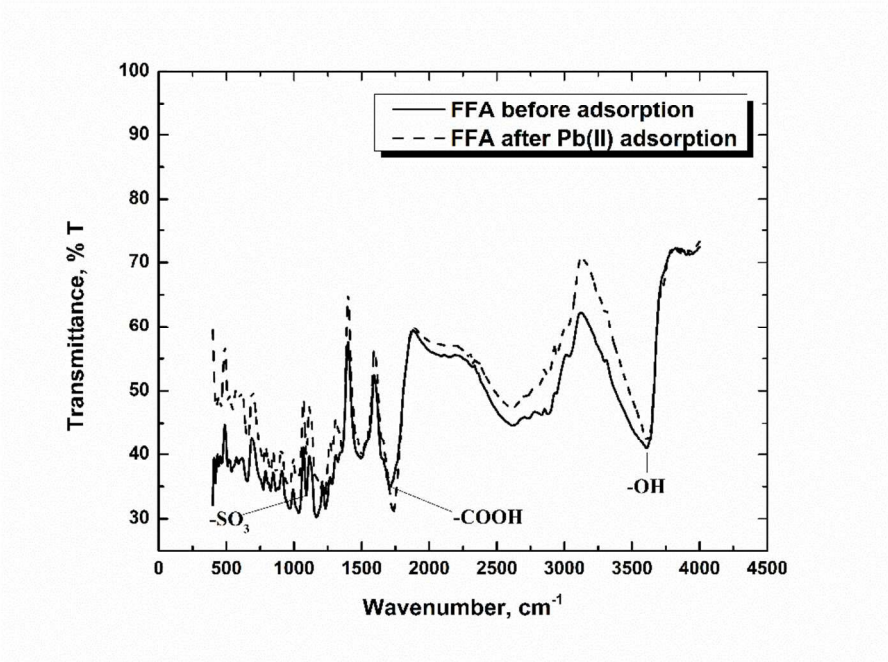

Fig. 2

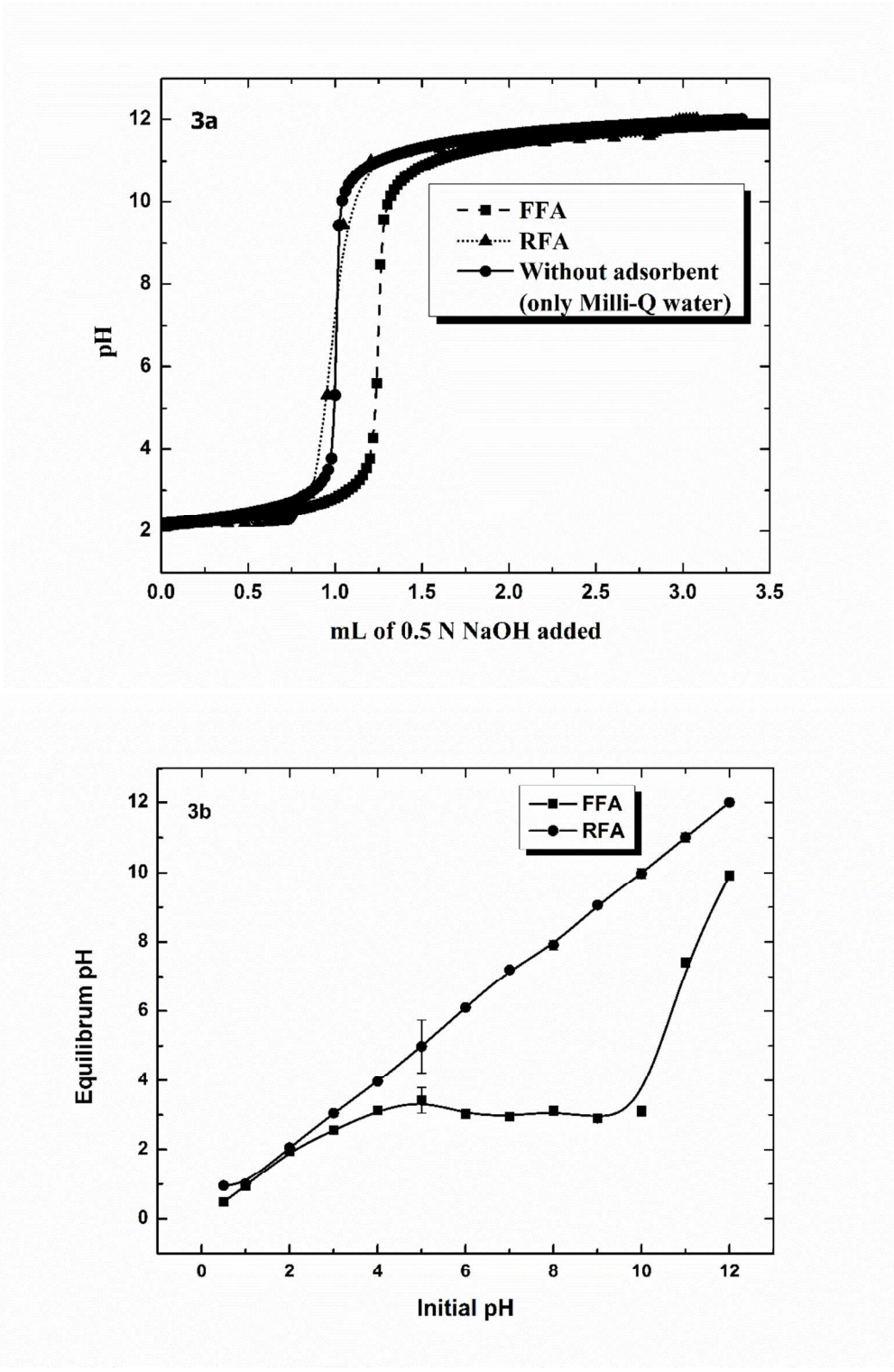

Fig. 3

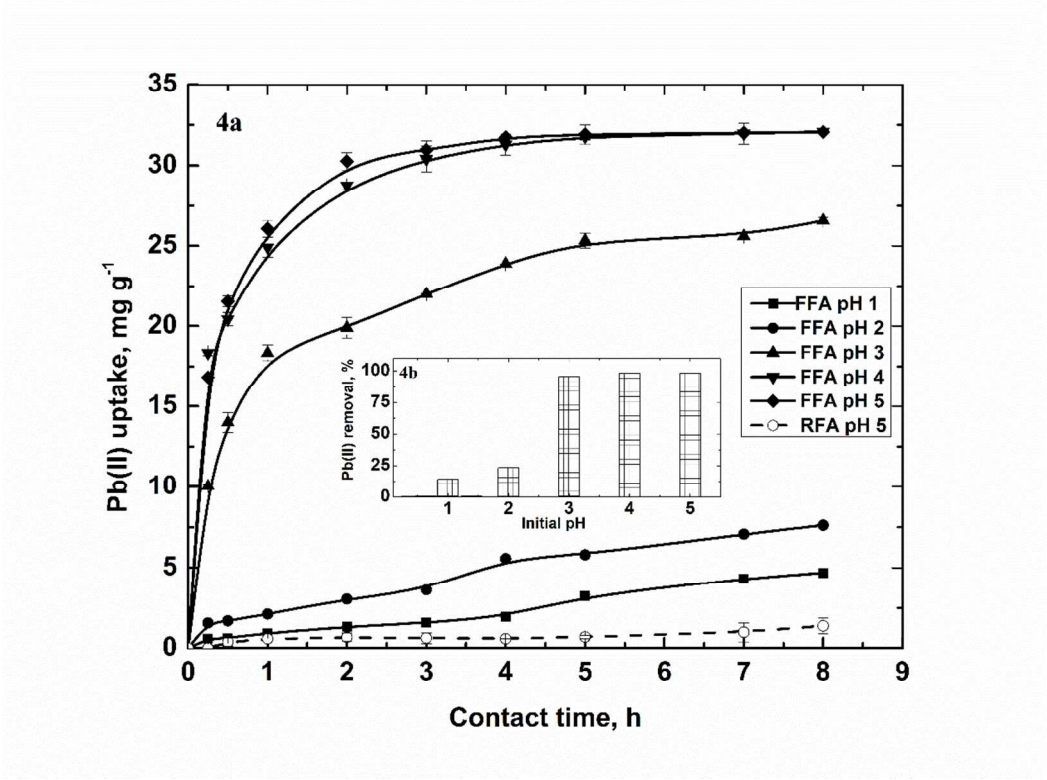

Fig. 4

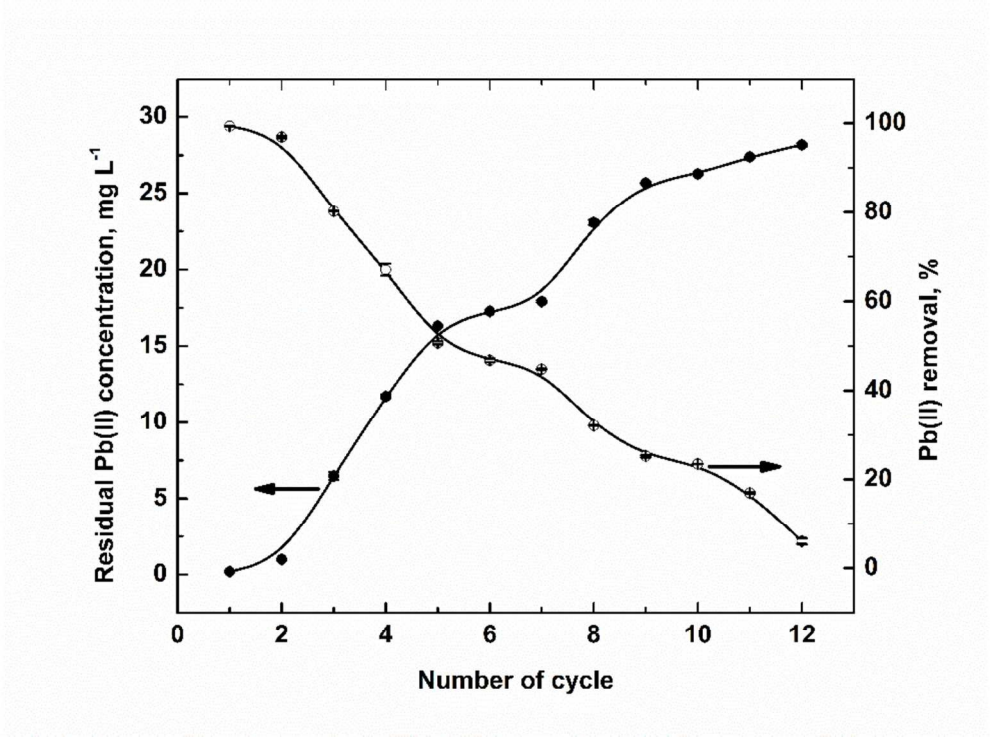

Fig. 5

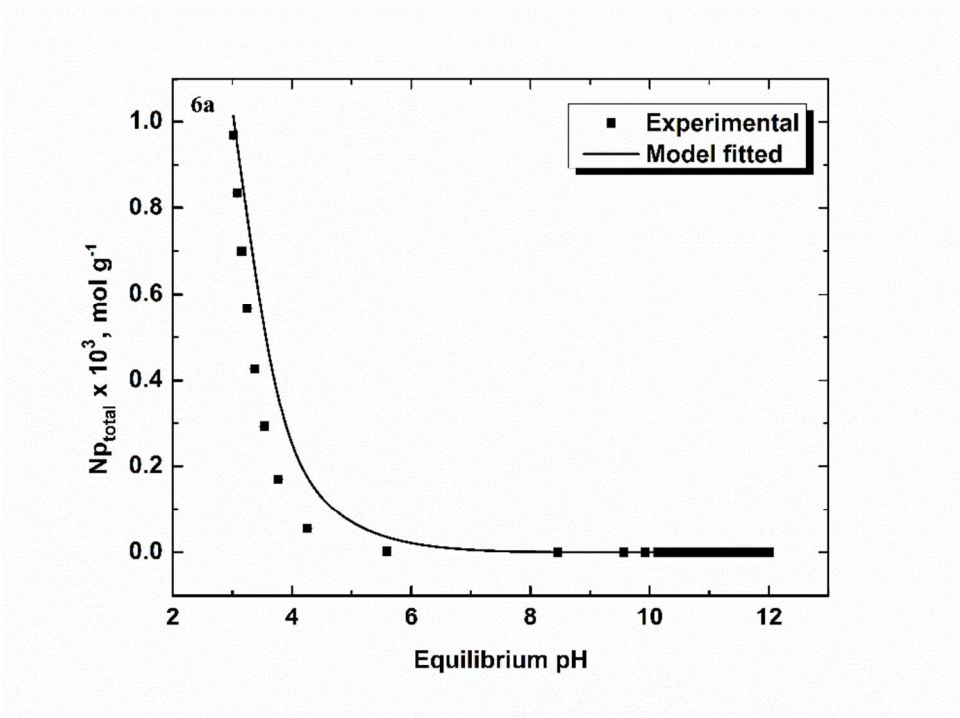

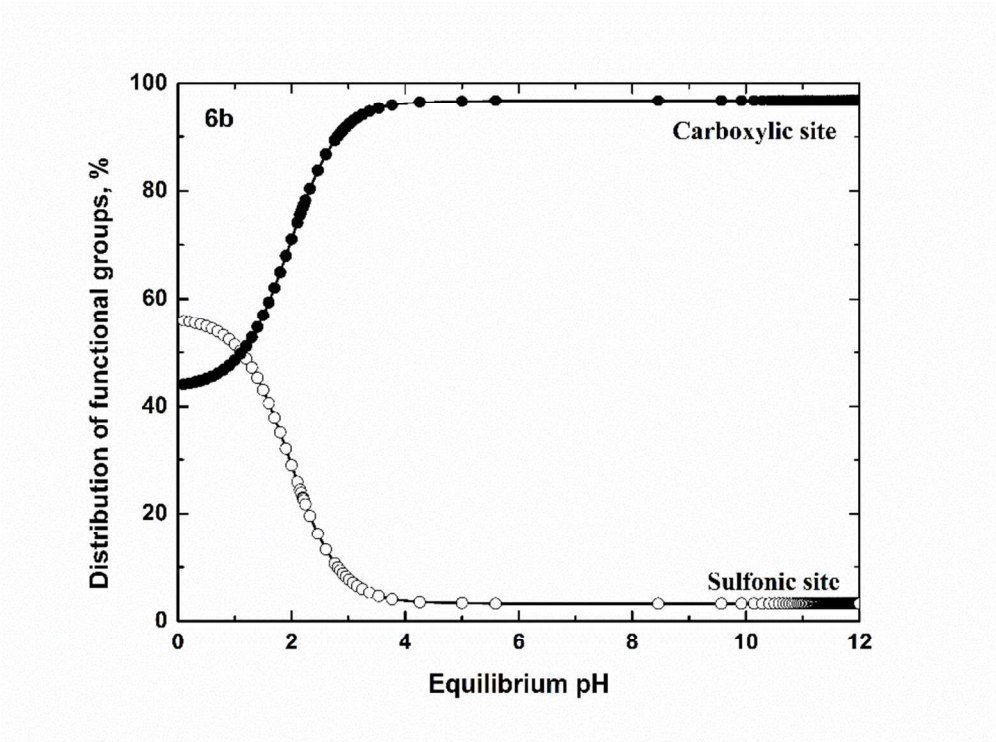

Fig. 6

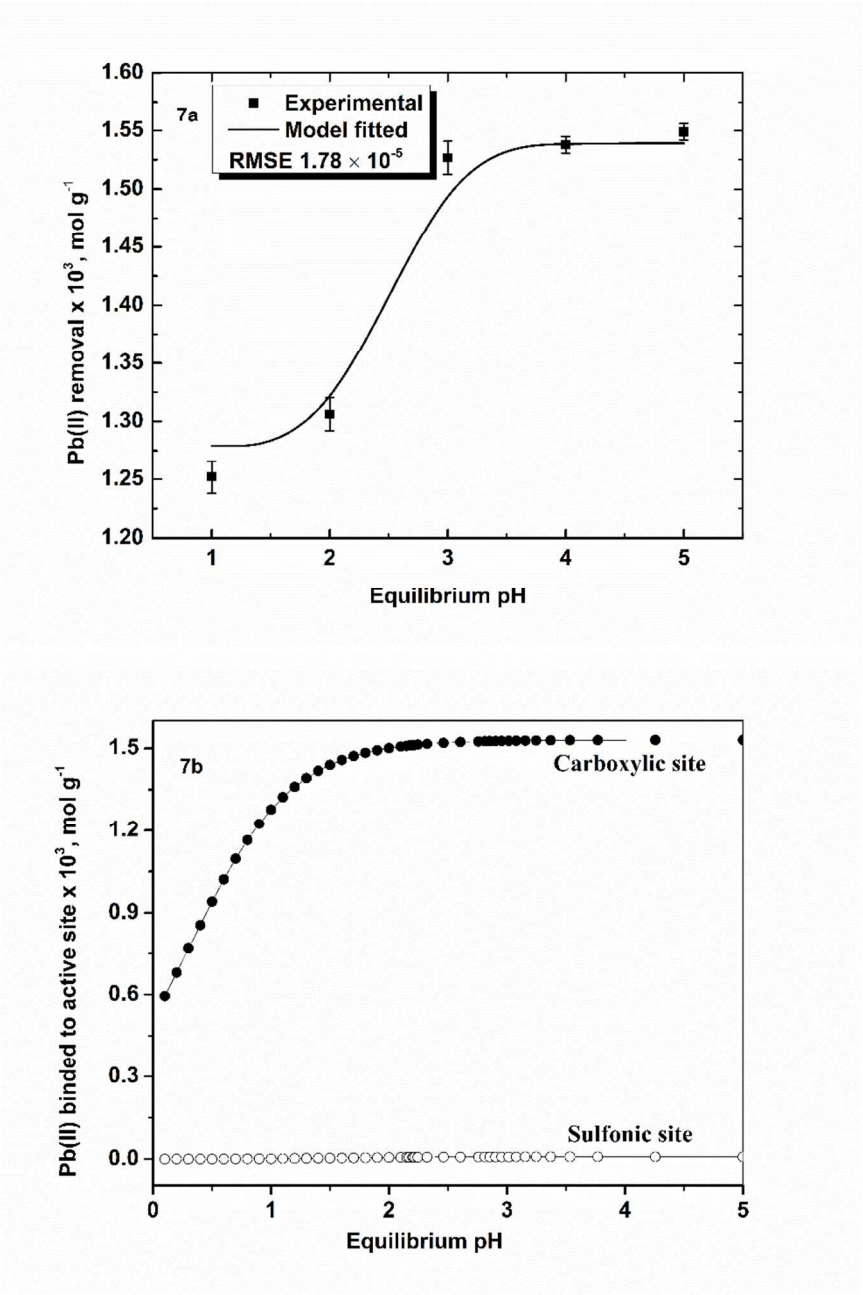

Fig. 7

Graphical abstract